Extended Abstracts of the 2014 International Conference on Solid State Devices and Materials, Tsukuba, 2014, pp356-357

Design and Growth of Nanowire Nanocavity

Toshihiro Wada[1], Shinjiroh Hara[1,2], and Junichi Motohisa[1]

[1] Graduate School of Information Science and Technology, Hokkaido University
[2] Research Center for Integrated Quantum Electronics, Hokkaido University
North 14, West9, Sapporo 060-0814, Japan, e-mail:wada@impulse.ist.hokudai.ac.jp

1. Introduction

Semiconductor nanowires (NWs) are attracting interest for applications in field-effect transistors (FETs), light-emitting elements, solar cells, and so on, due to their unique electrical and optical properties. We have been reporting on the controlled growth of V/III compound semiconductor NWs by selective-area metal-organic vapor phase epitaxy (SA-MOVPE) with diameter down to 30nm [1]. Such thin NWs are particularly important for FETs, but much thicker ones are beneficial for laser application to obtain large gain and Q-factors of the NW nanocavity [2,3]. However, the approach to realize thick NWs and, in particular, NW nanocavities with large Q-factors has rarely been explored so far. In this report, we describe the design of NW nanocavity to obtain large Q-factors. We also describe the growth of thick NWs by two-step growth in SA-MOVPE and their characterization.

2. Nanowire nanocavity design

To gain insight for the design NW nanociavity, electromagnetic (EM) fields in NW (with length L) were calculated by finite-difference time-domain (FDTD) simulation, and cavity modes and Q-factors were estimated. FDTD simulations were performed using a freely available software package [4]. For simplicity, the NW (refractive index n_{NW}=3.6) has a circular cross section with diameter d (or radius r), and the simulation is carried out assuming radial symmetry so that all the components of EM field is proportional to exp($im\phi$), where m is an azimuthal mode number and ϕ is the radial coordinate. Results of simulation are summarized in Fig.1 for d=460 nm and L=4 μm. Here, the number of nodes in one of the EM field components (E_z or H_z) is plotted as a function of cavity resonance wavelength λ_c by closed circles and solid lines. Note that the number of the nodes of the EM field is a measure of the longitudinal mode number l. It is also noted that the radial mode is also classified by introducing the integer n as a radial mode number. The size of the circles represents the magnitude of Q-factors, and is 2.2×10^4 for the mode (m,n,l)=(4,1,15) at λ_c=770nm. This result confirms that the NW can exhibit cavity modes with very larger Q-factors. The existence of such modes with larger Q-factors is previously addressed in Ref. [2], and is considered to be a hybrid one of whispering gallery modes and longitudinal modes of the Fabry-Perot cavity, or helical modes.

To know the resonance wavelength of hybrid modes is not trivial and requires rigorous calculations as we have described. However, we noticed that the all the resonance wavelength follows the propagation constant $\beta(\lambda)$ in a

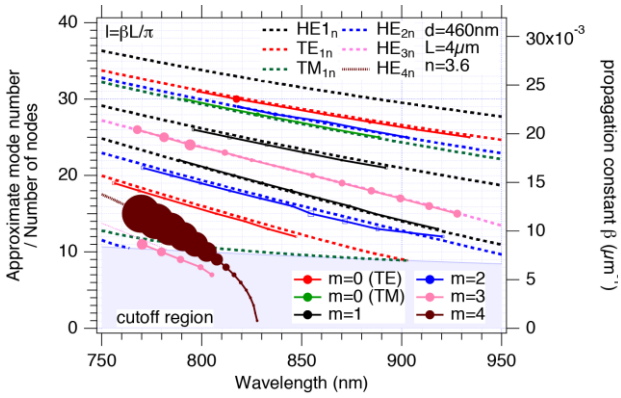

Figure 1: Resonance wavelength of NWs nanocavity and the dispersion relation of circular NW waveguide.

NW with infinite length. The dashed lines in Fig. 1 represents calculate $\beta(\lambda)$ for TE_{0n}, TM_{0n}, and HE_{mn} modes of a step-index fiber fiber with NW core and air cladding having circular cross sections. Specifically, the same curves show the relationship for the following approximate longitudinal mode number l:

$$l = L\beta(\lambda)/\pi \qquad (1)$$

This relationship closely follows the resonance wavelength λ_c, of each mode, as shown in Fig 1. Equation (1) is actually the resonance condition of the conventional Fabry-Perot cavity with length L if $\beta(\lambda)$ is replaced with the wavenumber k. Thus, approximate position of the resonance wavelength can be predicted by using Eq. (1). The deviation of the actual resonance wavelength from that obtained using Eq. (1) is due to the phase shift at the reflection at the NW edge, and can be estimated by using the method described in [5].

Our SA-MOVPE grown NWs have hexagonal cross sections, and it is expected that the mode with m=6 has similar properties in both circular and hexagonal NWs. The cutoff wavelength for the HE_{61} and HE_{62} modes are given

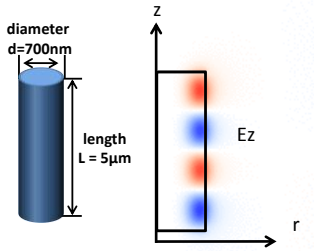

Figure 2: Intensity of the Ez-component of the EM field for the resonance mode with (m,n,l)=(6,1,3) for a circular NW with L=5 μm and d=700 nm.

by r/λ = 0.398 and 0.457, respectively. Thus, choosing the NW radius such that 0.398 λ < r < 0.457 λ is important to obtain hexagonal NW nanocavities with large Q-factors.

For-GaAs based NW, the emission wavelength is about 850 nm, thus we can get d of about 700nm. To confirm this, we calculated the resonance wavelength for NWs with d=700 nm and L=5 μm for m=6. One of the typical results is shown in Fig. 2, and we obtained Q = 1.64×10^5 for this mode (m, n, l)=(4,1,3) with λ_c = 845 nm.

3. Growth and characterization of thick NWs

In SA-MOVPE, the NW size can be controlled by the opening size d_0 of the mask, but the growth rate decreases drastically as d_0. To grow NWs with sufficiently large d and L, we carried out two-step growth [6]. We first grew GaAs NWs under growth condition A, in which the growth temperature T_G was 720°C and the partial pressure of AsH_3 [AsH_3] was 2.5×10^{-4} atm. The growth time was 20 or 30 min. Then, growth condition B, in which T_G was 570°C and [AsH_3] was 1.0×10^{-3} atm, was applied for lateral growth for 40 min. The partial pressure of TMGa [TMGa] was 2.7×10^{-6} atm for both conditions. The substrates for the SA growth is partially covered with SiO_2 and had periodic circular mask opening arranged in the triangular lattice. The diameter d_0 of the opening area was changed from 100 to 300 nm and the pitch a of the opening was changed from 0.75 to 5 μm. After the growth, size of the NWs was measured by secondary electron microscopy (SEM), and photoluminescence (PL) measurement on single NWs was conducted at 4.2K.

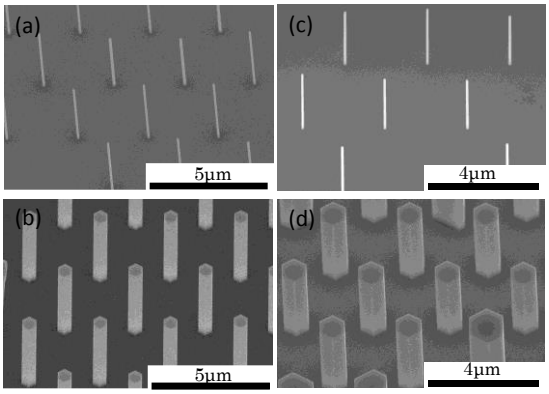

Fig. 3. SEM images of GaAs NWs, (a) After the 30 min growth with growth condition A. and (b) additional growth with condition B for 40 min. (c) After 20 min growth with condition A and (d) additional growth with condition B for 40 min.

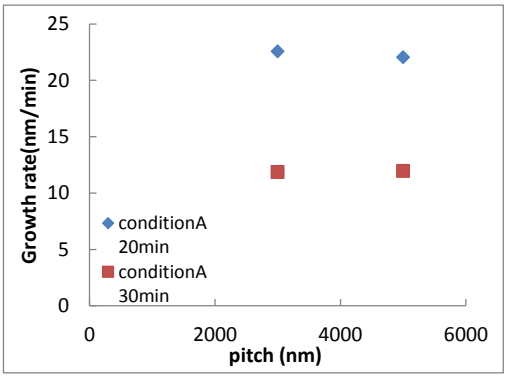

Figure. 4: The growth rate for the lateral growth in growth condition B.

Figures 1(a) and (c) show SEM images of GaAs NWs (NW-A and NW-C) with the growth condition A. The growth time was 30 and 20 min, respectively. The length L and the diameter d were L=4.28 μm and d=98.4 nm for NW-A and L=3.68 μm and d=92.9 nm for NW-C. The diameter of these NWs was nearly the same as the mask opening diameter d_0. Figures 1(b) and (d) (NW-B and NW-D) show the results of the second growth with growth condition B after the first growth with condition A for 30 and 20 min, respectively. Comparing NW-A (NW-C) and NW-B (NW-D), their diameter increases after the application of second growth, while the heights were almost unchanged. This indicates that the vertical growth is dominant for growth condition A and that the lateral growth is enhanced with growth condition B. The reason for the change in the growth mode is in the effective coverage of As atoms on the top (111)B and sidewall {110} surfaces[6]. Figure 4 shows the relationship between lateral growth rate and pitch a of the mask pattern. The lateral growth rate is independent of a but seems to be dependent of the length and diameter of the NW before growth.

Figure 5 shows PL spectra of NW-A and B. The emission intensity of NW-B was about 159 times as strong as NW-A, while volumes of NW-B was about 47 times as large as NW-A. This large enhancement of the emission intensity is mainly due to the reduced contribution of none-radiative recombination on the NW surface as d. At the same time, increased PL linewidth suggests the increased contribution of the cavity modes for larger d, which are now under investigation.

References

[1] Y. Kohashi *et al*., Appl. Phys. Exp. **6**, 025502 (2013).
[2] R. Chen *et al*., Nature Photon. **5**, 170 (2011).
[3] D. Saxena *et al*., Nature Photon. **7**, 963–968 (2013).
[4] A. F. Oskooi *et al*, Comp. Phys. Commun. **181**, 687 (2010).
[5] A. Maslov and C. Ning, Appl. Phys. Lett **83**, 1237 (2003).
[6] K. Ikejiri *et al*. J. Cryst. Growth **298,** 616–619 (2007).

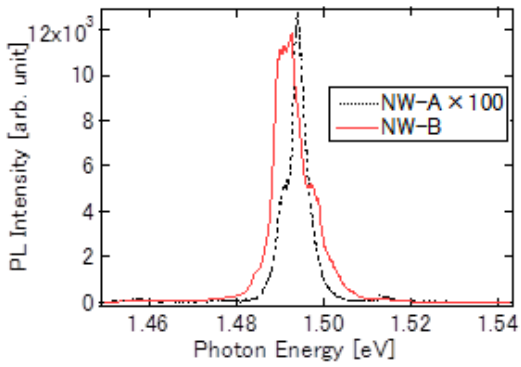

Fig. 5. PL spectra of GaAs NWs before and after the lateral growth.